CONTRAST MEDIA & MOLECULAR IMAGING

Received: 8 January 2014, Revised: 2 June 2014, Accepted: 4 June 2014, Published online in Wiley Online Library: 7 July 2014

(wileyonlinelibrary.com) DOI: 10.1002/cmmi.1613

Utilization of nanoparticles as X-ray contrast agents for diagnostic imaging applications

José Carlos De La Vega and Urs O. Häfeli*

Among all the diagnostic imaging modalities, X-ray imaging techniques are the most commonly used owing to their high resolution and low cost. The improvement of these techniques relies heavily on the development of novel X-ray contrast agents, which are molecules that enhance the visibility of internal structures within the body in X-ray imaging. To date, clinically used X-ray contrast agents consist mainly of small iodinated molecules that might cause severe adverse effects (e.g. allergies, cardiovascular diseases and nephrotoxicity) in some patients owing to the large and repeated doses that are required to achieve good contrast. For this reason, there is an increasing interest in the development of alternative X-ray contrast agents utilizing elements with high atomic numbers (e.g. gold, bismuth, ytterbium and tantalum), which are well known for exhibiting high absorption of X-rays. Nanoparticles (NPs) made from these elements have been reported to have better imaging properties, longer blood circulation times and lower toxicity than conventional iodinated X-ray contrast agents. Additionally, the combination of two or more of these elements into a single carrier allows for the development of multimodal and hybrid contrast agents. Herein, the limitations of iodinated X-ray contrast agents are discussed and the parameters that influence the efficacy of X-ray contrast agents are summarized. Several examples of the design and production of both iodinated and iodine-free NP-based X-ray contrast agents are then provided, emphasizing the studies performed to evaluate their X-ray attenuation capabilities and their toxicity *in vitro* and *in vivo*. Copyright © 2014 John Wiley & Sons, Ltd.

Keywords: computed tomography; multimodal imaging; contrast agents; hybrid contrast agents; X-ray attenuation properties; iodinated molecules; radiopaque elements; nanoparticles

1. INTRODUCTION

The prefix *nano*, which derives from the Greek *nanos* and means 'dwarf', describes materials, technologies or properties with dimensions on the nanoscale (10^{-9} m). The nanoscale represents the bridge between atoms and small molecules (10^{-10} m) and biological, chemical, mechanical and electrical microscopic entities (10^{-6} m). Nanotechnology is an interdisciplinary field that involves the study and application of natural sciences and engineering to develop tools at the nanoscale. Since its origins, which can arguably be traced to physicist Richard Feynman's lecture 'There's Plenty of Room at the Bottom' in 1959, nanotechnology applied to life sciences has led to improved knowledge about cellular and molecular processes and factors that cause or encourage a variety of diseases. The understanding of novel disease pathways has acted as a catalyst for the development of nanomedicine, an indisputably important research area within the scope of nanotechnology. Advances in this field promise to increase the accuracy and specificity of medical diagnoses and treatments of diseases characterized by the presence of severe and chronic pathologies. Unfortunately, for the majority of chronic degenerative diseases, effective treatments are only available for the initial disease stages. Hence, an early diagnosis is crucial to improve the survival rate of patients. Recently, nanoparticulate systems, mainly organic and inorganic nanoparticles (NPs), have found potential applications in different diagnostic imaging techniques because of their potential to target specific tissues and organs within the body. In this way, the region of interest can be highlighted, the overall efficiency of the procedure can be increased, and the side effects can be reduced.

Medical imaging aims to diagnose and examine diseases by creating images of the internal structures of the body. It also provides valuable information before starting an appropriate treatment and then following its efficacy. Among all the medical imaging technologies available, radiography is one of the most commonly utilized because it has a good spatial resolution (50–200 μm) and it requires a short time to complete the procedure (<10–15 min) (1,2). Radiography encompasses all the techniques that use X-rays, a form of ionizing electromagnetic radiation that can penetrate opaque substances (3), to generate contrast between different tissues and organs (4). X-ray imaging is based on the principle that X-ray photons are attenuated when they pass through the body. The total attenuation produced in the body is measured by a detector to create a two-dimensional (2D) image (5). A widely utilized modality of X-ray imaging is computed tomography (CT), a diagnostic tool that plays a pivotal role in the staging and imaging-guided intervention of various diseases owing to its noninvasive nature, high resolution and deep tissue penetration (6,7). In this technique, tomographic images (i.e. sectional images) are produced by processing a series of projections of the target tissues and organs taken from different angles (7). In modern CT scanners, a

* *Correspondence to: U. O. Häfeli, Faculty of Pharmaceutical Sciences, University of British Columbia, 2405 Wesbrook Mall, Vancouver, BC, V6T 1Z3, Canada. E-mail: urs.hafeli@ubc.ca*

J. C. De La Vega, U. O. Häfeli
Faculty of Pharmaceutical Sciences, University of British Columbia, 2405 Wesbrook Mall, Vancouver, BC, V6T 1Z3, Canada

Biographies

José Carlos De La Vega completed with honors a B.Sc. in Biotechnology Engineering with a Minor in Bioprocess Design and Bioseparation Science at the Monterrey Institute of Technology and Higher Education (ITESM) in Monterrey, Mexico in 2012. In 2011, he did a six-month professional internship in the Faculty of Pharmaceutical Sciences at the University of British Columbia (UBC) in Vancouver, Canada. His work involved the microfluidic production of uniformly sized polymeric microspheres for drug delivery applications. He is currently pursuing a Ph.D. degree in Pharmaceutical Sciences at UBC under the supervision of Dr. Hafeli. His research is focused on the production of rhenium-doped microspheres for diagnosis and treatment of hepatocellular carcinoma.

Urs O. Häfeli is currently an Associate Professor in the Faculty of Pharmaceutical Sciences at UBC. After receiving a B.Sc. degree in Pharmacy in 1986 and a Ph.D. in Radiopharmaceutical Sciences at the Federal Institute of Technology in Zurich, Switzerland in 1989, he spent 1.5 years as a postdoctoral fellow at the Joint Center of Radiation Therapy at Harvard University, followed by 11 years as a research scientist in the Radiation Oncology Department of the Cleveland Clinic Foundation. Dr. Hafeli is a leader in fighting cancer with radioactive pharmaceuticals and in the development of diagnostic imaging agents. He is also investigating the use of magnetic drug targeting and has been chairing an international conference in this field since 1996. Other active fields of nanomedicine research include the development and use of microneedles. Dr. Hafeli has over 80 peer-reviewed journal publications and holds 4 US patents.

three-dimensional (3D) reconstruction of the stack of transverse images can be performed to generate a volumetric image made up of voxels (8).

Owing to its high efficacy for imaging bone structure and acquiring high-resolution volumetric images in relatively short scan times (9), micro-CT (μCT) has developed over recent decades as a research tool. In broad terms, μCT refers to CT scanners that can resolve voxels with submillimeter spatial resolution (8,10). Nonetheless, a more appropriate generic term for this technique is microscopic CT, which can be further subdivided based on the spatial resolution into: mini-CT (200–50 μm), μCT (50–1 μm) and nano-CT (1–0.1 μm) (8) (Fig. 1).

In both medical research and clinical practice, contrast agents must be utilized in all different modalities of CT imaging, including fluoroscopy (5,11), to enhance the visibility of tissues and organs, as soft biological tissues lack sufficient contrast (12). However, a problem with clinically used contrast agents is that they only provide limited contrast, which can lead to inaccurate diagnoses (4,12). For example, imaging of small blood vessels is, in the majority of cases, very poor and, therefore, detection of vascular angiogenesis, which is critical to achieve an early diagnosis of cancer, remains a challenge (12). As a matter of fact, other medical imaging techniques, such as magnetic resonance imaging (MRI), positron emission tomography (PET), single photon emission computed tomography (SPECT) and optical imaging face the same problem. Despite the differences between them, the use of multimodal imaging agents makes it possible to combine some of these techniques into a single scan to enhance the accuracy of diagnoses by utilizing information obtained from each one (13,14). As multimodal imaging usually involves the use of at least one X-ray imaging technique (15,16), the development of contrast agents with enhanced X-ray attenuation capabilities is currently an actively pursued area of research. Thus, several efforts are focused on the design of X-ray contrast agents at the nanoscale. One of the most prevalent strategies is the encapsulation of elements with high linear or mass X-ray absorption coefficients into NPs. Herein, we aim to review and analyze the evolution of X-ray contrast agents from small molecules to nanoparticulate systems and the different strategies to design and evaluate these NPs.

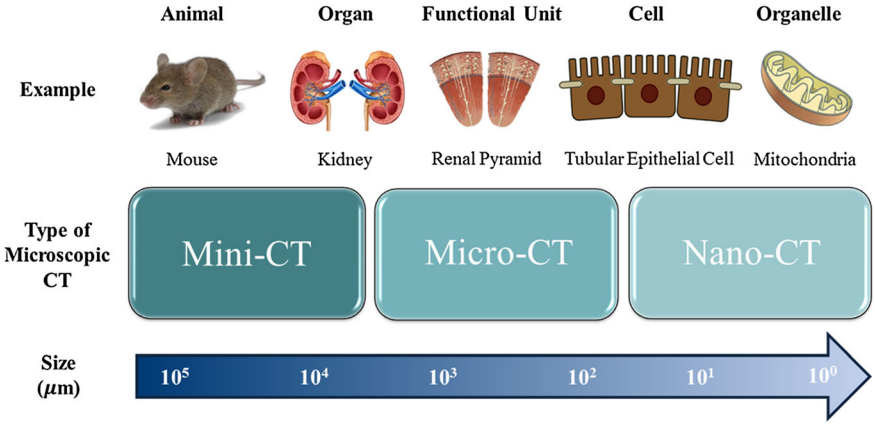

Figure 1. Types of microscopic CT. While all three types operate on the same physical principles, it is their distinct spatial resolution that determines what example can be successfully imaged.

2. OVERVIEW OF X-RAY CONTRAST AGENTS

Owing to significant progresses in molecular and cell biology related to the identification of specific cell targets, it is now possible to perform diagnostic and molecular imaging studies with a high degree of accuracy and specificity (2,17). Advances in this field promise to facilitate early diagnosis, identify the stage of a disease and provide fundamental information about pathological processes, so that diagnostic and molecular imaging could also be applied to follow-up the efficacy of a specific therapy (11,17). One way of enhancing the efficiency of imaging studies is the development of improved X-ray contrast agents, which are molecules commonly used in radiographic procedures to ensure a high image contrast based on the strong X-ray attenuation properties of radiopaque elements (18). Given that X-rays have a short wavelength, which is in the range of 0.1–10 nm (19,20), they can detect subtle differences in the electron density of a material which are not visible using other absorption-based techniques (20). Therefore, X-rays are excellent tools to study biological tissues (21). In the following section, an overview of the characteristics of conventional X-ray contrast agents is given, emphasizing their limitations. Then, novel X-ray contrast agents under development meant to overcome the drawbacks associated with clinically used X-ray contrast agents are described in detail.

2.1. Iodinated X-Ray Contrast Agents

Currently, X-ray contrast agents are predominantly based on small iodinated molecules. Iodine (I) took the leading role in X-ray contrast agent synthesis because of its high mass X-ray absorption coefficient [1.94 $cm^2\ g^{-1}$ at 100 keV (22)] and its chemical versatility. This specific property is evident from the development of iodinated X-ray contrast agents, which moved from inorganic iodine (e.g. NaI) to organic mono-iodinated (e.g. uroselectan A), di-iodinated (e.g. uroselectan B) and tri-iodinated (e.g. diatrizoate) molecules, from lipophilic to hydrophilic molecules, from ionic to nonionic (e.g. iohexol, iopromide and iopamidol) molecules, and from monomers to dimers (e.g. iotrolan) (18) (Fig. 2).

The evolution in the structure of the iodinated X-ray contrast agents intended to reduce the adverse effects associated with the clinical use of these molecules. For example, nonionic molecules have a lower tendency to interact with cell membranes, peptides and other biological structures, so that they are less toxic than ionic molecules (19). Dimers show lower osmolalities than monomers, which reduces pain and sensation of heat at the site of injection (19,23,24) and decreases the incidence of contrast media-induced nephrotoxicity (CMN), which is a common condition in patients with pre-existing renal impairment (23,24), cardiovascular complications (i.e. heart rate and blood pressure irregularities) and osmotic diuresis (18). Nevertheless, dimers tend to exhibit higher viscosities than monomers (19), which is something of concern because the higher the viscosity of the X-ray contrast agent is, the slower the rates of injection and excretion are (23). Additionally, slow excretion rates have been associated in preclinical studies with upregulation of markers for renal injury (25). This situation usually limits the use of dimers in CT and angiography imaging, as these techniques require high injection rates (i.e. up to 20 mL s^{-1}) (23,24). Iodinated X-ray contrast agents with a high osmolality and viscosity are normally administered intravascularly by either intra-arterial injection, which requires the use of catheter, or intravenous injection. Nonetheless, this route of administration has been reported to increase the risk of CMN and anaphylactoid reactions. For this reason, when possible, the enteric and direct (e.g. percutaneous injections) routes of administration are preferred (26). Hence, a balance between osmolality and viscosity values must be found for each X-ray contrast agent under development.

Despite the efforts made to improve the physicochemical properties of iodinated X-ray contrast agents, those that are currently commercially available [e.g. Omnipaque™ (iohexol, a nonionic monomer), Visipaque™ (iodixanol, a nonionic dimer) (23)] still impose serious limitations on medical imaging. For instance, these molecules are usually rapidly excreted by the kidneys, limiting their application in several imaging techniques and triggering serious adverse reactions as a consequence of the large and repeated doses that are usually required (6). Moreover, one of the biggest concerns about the utilization of iodinated X-ray

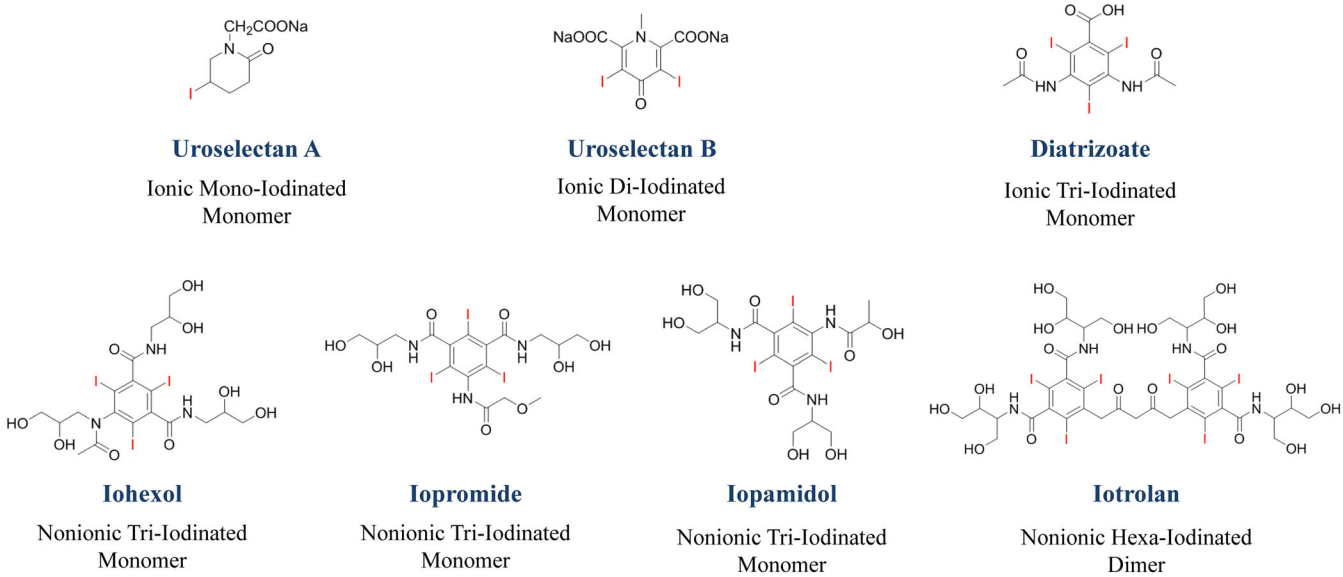

Figure 2. Chemical structure of representative iodinated X-ray contrast agents. The development of iodinated X-ray contrast agents moved from both inorganic and organic, lipophilic, ionic molecules to organic, hydrophilic, nonionic molecules. Additionally, to enhance the contrast obtained, dimers are preferred over monomers.

contrast agents is related to the fact that they have a greater density than plasma, resulting in an extreme hyperosmolarity (27). The incidence of both acute (i.e. within an hour) and delayed (i.e. within an hour and a week) adverse reactions is higher after the utilization of high-osmolarity iodinated X-ray contrast agents. Acute adverse reactions can range in severity from mild to severe and life-threatening and are directly related to the chemotoxicity, the ionic state (i.e. ionic or nonionic), the viscosity and the osmolarity of the formulation. Several cohort studies have shown that common signs and symptoms are anaphylaxis, arrhythmia, vasovagal responses (manifested as bradycardia with hypotension), hemodynamic changes, nausea and emesis. Delayed adverse reactions, however, tend to be milder in nature. They mostly include cutaneous reactions (e.g. rash and pruritus), which are thought to be caused as a response of the immune system to the formulation (26).

As a result of the inherent limitations of the X-ray contrast agents based on small iodinated molecules, an active field of research is the development of alternative X-ray contrast agent formulations, most of them using NPs to enhance the efficacy of the contrast-generating materials. However, in order to determine whether or not they are suitable for diagnostic imaging applications, an accurate evaluation of their properties must be performed.

2.2. Characterization of Novel X-Ray Contrast Agents

The development of a novel X-ray contrast agent from the synthesis of the compound to the product license can take several years. During this period, the tolerance of the X-ray contrast agent must be rigorously tested to establish a safety and efficacy profile for the formulation (28). Even though both the X-ray attenuation properties and the toxicity of the newly synthesized compounds are always evaluated during this process, it is clear from the historic development of iodinated X-ray contrast agents that their physicochemical properties are equally as important for *in vivo* applications and, thus, should also be assessed. The most important parameters that need to be taken into account in the appraisal of novel X-ray contrast agents are schematically shown in Fig. 3. A great deal of feedback is required during these studies because, even if a compound is an excellent candidate in terms of its physicochemical properties, this does not imply, in all cases, that it will exhibit suitable X-ray attenuation properties or that it will be safe for administration into the body, and vice versa.

The physicochemical properties of X-ray contrast agents are particularly important in guiding the search for improved molecules because they determine to a great extent their pharmacological and toxicological behavior (18). Among them, the atomic number (Z), which is related to the capability of an element to attenuate an X-ray beam, is the most important one in the generation of contrast. Although the attenuation process is the result of both the absorption and the scattering of light, it is useful to focus only on the linear X-ray absorption coefficient, as its relationship with the atomic number is direct. For this reason, the linear X-ray absorption coefficient is sometimes referred to as the linear X-ray attenuation coefficient. Basically, the linear X-ray absorption coefficient is a measure of the fraction of an X-ray beam that is absorbed per unit thickness of the absorber material at a specific energy. This phenomenon is indeed described by eqn (1), which is an integrated form of the Beer–Lambert law and is valid in the case of narrow beams of mono-energetic photons (29).

$$I = I_0 e^{-\mu d} \tag{1}$$

where I is the intensity of the transmitted X-ray radiation, I_0 is the intensity of the incident X-ray radiation, μ is the linear X-ray absorption coefficient, and d is the thickness of the irradiated sample (29). Furthermore, the linear X-ray absorption coefficient, which has units of reciprocal length, is a function of the X-ray energy and the physical and the chemical properties of the sample, as demonstrated in eqn (2) (19).

$$\mu \approx \frac{\rho Z^4}{A E^3} \tag{2}$$

where E is the X-ray energy and ρ and A are the density and atomic mass of the element, respectively (19). However, to compare between different chemical species, the mass X-ray absorption coefficient (μ/ρ), which is calculated by dividing the linear X-ray absorption coefficient by the density and, therefore, has units of length squared per mass, is commonly reported. In summary, the higher the atomic number, the better the absorption of X-rays and, thus, the X-ray attenuation properties. For this

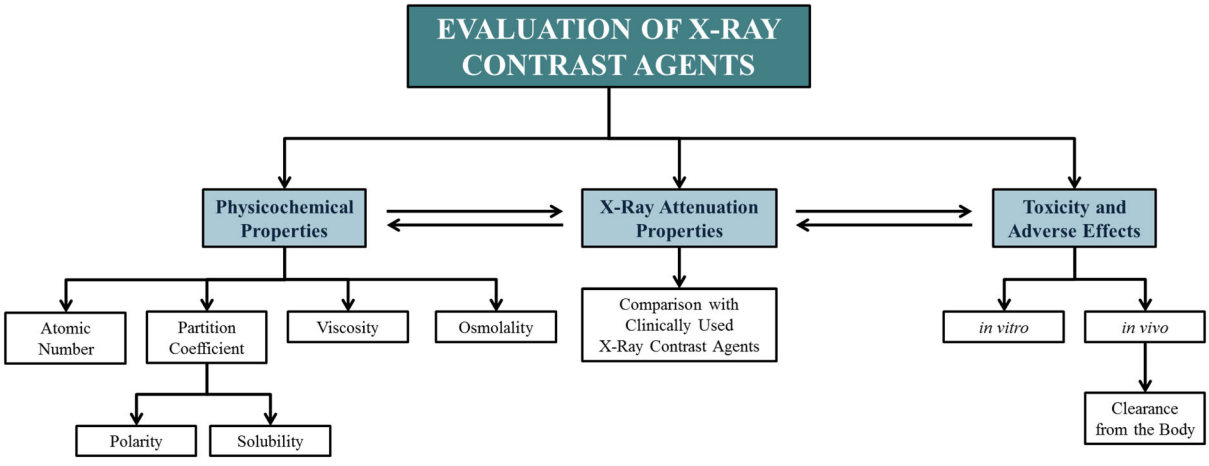

Figure 3. Schematic representation of important parameters in the evaluation of novel X-ray contrast agents. The diagram shows the parameters that need to be evaluated in order to characterize a novel X-ray contrast agent and determine whether or not it is suitable for diagnostic imaging applications.

reason, most of the current research is focused on the replacement of iodine with elements having appreciable higher atomic numbers. However, an increase in atomic number is, in the majority of cases, associated with potential toxicity and possible accumulation of the X-ray contrast agent in tissues and organs (30,31), underlining the importance of conducting a complete evaluation of the properties of the compound.

Although no clear-cut structure–activity relationships exist, allergy-like events (e.g. nausea and emesis) are usually related to the use of lipophilic X-ray contrast agents (18). Regarding the final formulation of the X-ray contrast agent, it is crucial to decrease its viscosity and osmolality. The first term, viscosity, describes the ability of the formulation to flow and is strongly influenced by the concentration of the radiopaque element and the temperature of the solution (18). Basically, highly viscous X-ray contrast agents limit the rate of injection and might cause pain at the site of injection (23,24). The second term, osmolality, is proportional to the number of particles in the solution and causes the major concerns in the use of novel X-ray contrast agents. The adverse effects related to an increase in osmolality include mainly cardiovascular complications and osmotic diuresis. In general, the closer the osmolality of an X-ray contrast agent is to the plasma osmolality, the lower the incidence of side effects. For this reason, X-ray contrast agents are usually classified into: high osmolar agents (i.e. osmolalities in the order of 1500 mosm kg^{-1}), low osmolar agents (i.e. 600–700 mosm kg^{-1}) and isotonic agents (osmolalities similar to the plasma osmolality, which is around 300 mosm kg^{-1}) (18).

The current strategy to evaluate the efficacy of novel X-ray contrast agents is to compare the X-ray attenuation that they produce relative to clinically used iodinated X-ray contrast agents (30,32–34). When the results of this comparison are favorable, both *in vitro* and *in vivo* studies must be conducted to determine whether or not the newly synthesized compound can be utilized for medical applications. Additionally, *in vivo* studies are highly important in order to characterize the biodistribution and clearance from the body of the X-ray contrast agent. A complete and accurate characterization and evaluation of the X-ray contrast agent under development needs to include all the aforementioned parameters.

To improve the physicochemical properties and reduce the toxicological effects, the recent trend is to protect the radiopaque element via encapsulation into a suitable carrier. Owing to the several advantages related to the use of nanotechnology for medical applications, these carriers are usually designed at the nanoscale. In addition to the NPs described herein, which, unless otherwise stated, are spherical, organic or inorganic nanocarriers, there is plenty of literature regarding the development and utilization of liposomes, micelles and dendrimers as X-ray contrast agents. First, liposomes are self-assembled vesicles of phospholipids that enclose a hydrophilic core (7,35). Therefore, liposomes can be used to deliver both hydrophobic molecules (dissolved in the phospholipid bilayer) and hydrophilic molecules (entrapped in the core) (35). Second, micelles are self-assembled colloidal-sized clusters made from either surfactants (surfactant micelles) or amphiphilic di- or tri-block copolymers (polymeric micelles) (36). They are spontaneously formed when the concentration of surfactant or block copolymer is above the critical micelle concentration (37) and they have a hydrophobic core and a hydrophilic shell or corona in aqueous environments (38). As opposed to liposomes, micelles are used to deliver only hydrophobic molecules (35,38). Finally, dendrimers are well-controlled and well-defined complexes comprising branched polymers. They are typically symmetric around the core and adopt a predictable spherical 3D structure (7,35). The dendrimer architecture is highly advantageous because it comprises three regions: a core, several internal layers of repeating units (known as generations), and a surface that ultimately determines the macroscopic properties of the dendrimer. Basically, the core and the generations can be used to dissolve small molecules and the surface can be functionalized to expose desired chemical moieties (7).

To date, only iodine-containing liposomes, polymeric micelles and dendrimers have been evaluated for X-ray imaging applications. Initially, the approach for the development of iodinated liposome-based X-ray contrast agents was the encapsulation of clinically used iodinated X-ray contrast agents into the liposomes for imaging of the spleen (39) and the liver (40). Now, after the emergence of long-circulating liposomes coated with poly(ethylene glycol) (PEG), it is also possible to image other organs to study and diagnose chronic diseases (41,42). The strategy for the development of iodinated polymeric micelle-based and dendrimer-based X-ray contrast agents is the reaction of iodinated benzoic acids with amine or hydroxyl groups in the polymer chains (35). For example, some groups have prepared polymeric micelles and dendrimers using block copolymers comprising iodine-substituted poly-L-lysine (36,43–46).

Nonetheless, current research has moved towards the utilization of NPs constituted of either natural polymers (e.g. alginate, chitosan and collagen) or synthetic polymers made from naturally occurring monomers, such as lactic acid and glycolic acid (47). These nanocarriers are very versatile because of the large number of polymers available, which in turn provides flexibility to design NPs with different physical and chemical properties, particularly those related to their size, size distribution, stability and predictable biodegradation rate. This review focuses precisely on this type of NPs, which have been utilized to evaluate the contrast enhancement of various elements, including iodine. In the following section, the benefits associated with the design of NP-based X-ray contrast agents and their main characteristics are summarized and discussed. Different examples of these novel X-ray contrast agents are also provided, emphasizing, in each case, the studies that have been done to demonstrate their potential applications in diagnostic and molecular imaging.

3. NANOPARTICLE-BASED X-RAY CONTRAST AGENTS

The development of NP-based X-ray contrast agents is providing an increasing contribution to the field of diagnostic and molecular imaging. An ideal contrast agent should selectively accumulate at the site of interest to be able to interact physically, chemically, biochemically and functionally with the target and, by these means, improve the image contrast (48). The utilization of NPs provides several advantages over the widely used iodinated contrast agent solutions. For example, their surface can be modified to enhance their specificity by attaching targeting moieties (48,49), increase their circulation half-life by adding appropriate coatings (e.g. polymers, silica) (48–50) and improve their functionality by adding other components, including fluorescent markers and therapeutic agents (11,48,51) (Fig. 4). The integration of both contrast and therapeutic agents in a single carrier is known as theranostics (11,51). Theranostic medicine promises to develop NPs capable of, first, diagnosing via imaging studies;

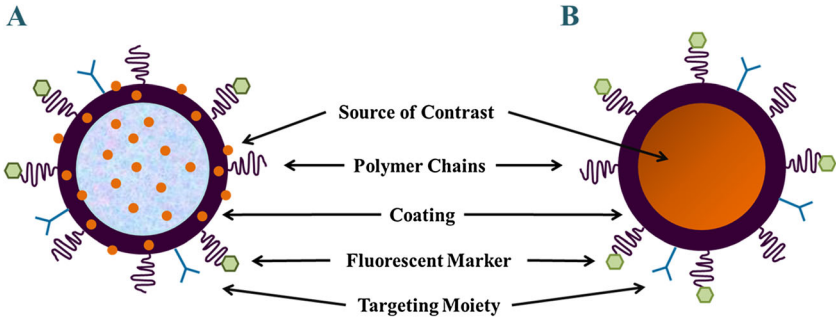

Figure 4. Generalized representation of the different strategies to design NP-based X-ray contrast agents. The NPs can be functionalized by adding polymer chains, suitable coatings, fluorescent markers and/or targeting moieties. The source of contrast can be either (A) a polymer-based NP in which the radiopaque element is loaded into the core, included within the coating or attached to the surface or (B) an inorganic NP made from an element that exhibits X-ray attenuation properties.

second, delivering drugs in a targeted way; and third, monitoring the response to the therapy (51), all with the same agent.

These types of 'smart' NP-based X-ray contrast agents are becoming increasingly important because they incorporate an appropriate radiopaque element, targeting ligands, a biocompatible coating and, in some cases, a therapeutic functionality. As a result, they exhibit an intense and stable output and tunable biodistribution profiles (6). Another advantage of the use of NPs as X-ray contrast agents is that they contain a high payload of the contrast-generating material, which increases the number of atoms of the radiopaque element that are delivered to the target and also facilitates the detection and follow-up upon administration (49). The contrast-generating material, which is usually an element with a high X-ray absorption coefficient bound to different ligands, can be located in the core, the coating or the surface of a polymeric NP (11) (Fig. 4A). This approach provides the flexibility of including multiple radiopaque elements and/or combine contrast and therapeutic agents within the same NP (11). The addition of more than one source of contrast increases, for example, the range of energies at which the NPs can be imaged with high resolution and, at the same time, facilitates biodistribution studies via multimodal imaging techniques (11,48). However, a different approach is to synthesize inorganic NPs made from an element that exhibits good X-ray attenuation properties and functionalize their surface to increase their stability *in vivo* (48) (Fig. 4B). Moreover, the characteristic high surface area-to-volume ratio of the NPs is advantageous in order to add a high number of ligands (i.e. peptides, proteins, antibodies, aptamers) to their surface, allowing specific recognition by biological targets within the body (52).

The biological stability and the geometric volume of the NPs are two important considerations during the first stages of NP-based X-ray contrast agent development. A common strategy to adequately stabilize the NPs *in vivo* is the modification of the surface with PEG or thiolated PEG (PEG-SH). These surface ligands increase the hydrophilicity of the NPs and enhance the circulation half-life by blocking the adsorption of serum proteins and opsonins that facilitate uptake and excretion by cells of the mononuclear phagocyte system (MPS) (53). Considering the number of functionalities that can be incorporated, the NP size becomes a critical parameter. For example, an NP with not only imaging, but also targeting functionalities requires a diameter of at least 20 nm. This is approximately the diameter of a ribosome, which, analogously, has several recognition and effector sites. For molecular imaging, which aims to understand the cellular function and follow-up molecular pathways and processes, NPs $<$150 nm are preferred because they can easily undergo endocytosis. On the one hand, 10–30 nm NPs are engulfed into the cells by clathrin-mediated endocytosis given that the endocytotic vesicles are 40–60 nm in size. On the other hand, 30–150 nm NPs are taken up by clathrin-independent endocytosis and, thus, they pass through the claveolae (invaginations of the cell membrane) (54). For other imaging applications, well-stabilized NPs up to 500 nm in size are typically used because they selectively accumulate at tumors sites as a result of the enhanced permeability and retention (EPR) effect, which describes the abnormal form and architecture of the tumor neovessels, often described as 'leaky'. This opposes to the fast kidney clearance of small molecules and the phagocytosis of micrometer-sized particles by cells of the MPS (53,55).

Owing to their numerous advantages, many different NP-based X-ray contrast agents have been designed. Some of the first attempts to use NPs as X-ray contrast agents used iodine as the radiopaque element. The utilization of NPs reduces the toxicity observed when iodine molecules are directly administered into the body (31). Nevertheless, it has also been evident that other elements possess interesting X-ray attenuation properties and, thus, there is an increasing trend towards the use of iodine-free NP-based X-ray contrast agents. In the following sections, the advantages and disadvantages of these two groups of novel NP-based X-ray contrast agents are discussed.

3.1. Iodinated Nanoparticle-Based X-Ray Contrast Agents

The most common approach to prepare iodinated NP-based X-ray contrast agents is to covalently bind iodinated moieties to a polymer backbone and then force the formation of the NPs by preparing an emulsion (56,57), which can be done using a wide variety of well established techniques. This strategy is highly advantageous because it prevents leakage and loss of the contrast agent material (i.e. the iodinated molecule) from the NP. In addition, as there are many different polymers available, it is feasible to design X-ray contrast agents with specific properties and functionalities (19). Recently, this approach has been successfully utilized to produce iodinated NPs by either emulsion polymerization (56) or nanoprecipitation (57).

The first method, emulsion polymerization, was used to synthesize iodinated copolymeric NPs of 2-methacryloyloxyethyl (2,3,5,-triiodobenzoate) (MAOETIB) and glycidyl methacrylate (GMA), an ester of methacrylic acid, with a hydrodynamic diameter of 50.0 $\pm$ 7.6 nm (56) (Fig. 5). As the P(MAOETIB-GMA) NPs were shown to be stable against agglomeration in an aqueous solution,

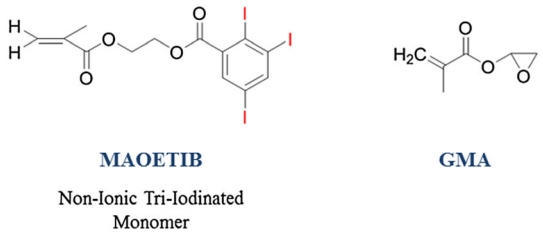

Figure 5. Chemical structure of 2-methacryloyloxyethyl(2,3,5,-triiodobenzoate) (MAOETIB) and glycidyl methacrylate (GMA). An iodinated NP-based X-ray contrast agent stable both *in vivo* and *in vitro* was prepared by emulsion copolymerization of MAOETIB and GMA.

they were tested *in vivo*. Following intravenous administration in rats, CT imaging revealed a significant enhanced visibility of the blood pool. The lymph nodes, the liver and the spleen were only seen after 30 min, when uptake by cells of the MPS took place. Furthermore, after intravenous administration in mice bearing hepatic cancer, it was seen that visual enhancement of healthy liver tissue increased gradually owing to the high uptake of the NPs by cells of the MPS, such as Kupffer cells. However, the NPs were not taken up by tumor cells because they displace macrophages, including Kupffer cells. As a consequence of this, liver tumor is favorably delineated as the dark nonenhanced regions within the healthy liver tissue. Hence, P(MAOETIB-GMA) NPs might be useful for the diagnosis of hepatic cancer (56).

The second method, nanoprecipitation, was used to prepare iodinated cellulose acetate NPs with a mean diameter of 79 nm (57). The advantages of using cellulose acetate rely on its biocompatibility, biodegradability and enhanced solubility over cellulose in organic solvents, which improve the overall throughput of the nanoprecipitation technique. A radiopacity study performed in a PET scanner equipped with an X-ray tube operating at 130 kVp demonstrated that the iodinated cellulose acetate NPs exhibited good X-ray attenuation properties. The NPs, suspended in an aqueous solution, maintained their morphology and proved to be stable after 3 months of storage at room temperature. Additionally, they were also successfully loaded with paclitaxel, indicating that these NPs can potentially be used as theranostic agents (57). Given the simplicity of this method, this type of NPs can be easily used for medical applications. However, toxicity and cellular uptake studies need to be performed first.

A different strategy from covalently binding iodine is to physically entrap iodinated molecules into polymeric carriers. Nonetheless, to date, only the production of microspheres has been reported (31). Basically, poly(vinyl)alcohol (PVA) microspheres loaded with iopamidol were prepared by a simple homogenization process. The microspheres had a mean diameter from 1.0 to 5.0 μm depending upon the specific concentrations of reagents utilized. An *in vitro* toxicity study in A549 human lung carcinoma cells showed that these microspheres have a good safety profile and are stable in water over a long period of time. Moreover, an X-ray imaging experiment conducted in a synchrotron showed that these iopamidol-loaded microspheres exhibit an X-ray attenuation profile comparable to that of iopamidol at equivalent iodine concentrations (31). This work represents a pioneering contribution to the development of a new generation of iodinated X-ray contrast agents. As toxicological effects are minimized after encapsulation of the iodinated molecules (31), the development of similar polymeric carriers at the nanoscale should be commenced.

3.2. Iodine-Free Nanoparticle-Based X-Ray Contrast Agents

A current area of active research is the development of inorganic NP-based contrast agents. Unlike the NPs described in the previous section, in which iodinated molecules are covalently bound to polymer chains, inorganic NP-based contrast agents comprise an inorganic core that exhibits imaging properties. Hence, they contain a large number of radiopaque atoms in a relatively small volume, which allows for intravenous administration at low concentrations, especially if the NPs are targeted by the addition of biological recognition moieties to the surface (52). So far, the most important advancements in this field are the development of quantum dots, magnetic NPs and NPs containing high atomic number elements.

In broad terms, quantum dots are inorganic NPs made from hundreds to thousands of atoms of elements of the groups II and VI (e.g. CdSe and CdTe) or groups III and V (e.g. InP and InAs) (58). They usually have mean diameters of $<$10.0 nm (19) and exhibit size- and composition-tunable optical absorption/emission properties over a wide spectral range that encompasses visible and infrared wavelengths (19,59). Magnetic NPs, which are also inorganic NP-based X-ray contrast agents, enhance the proton relaxation of specific tissues and are usually made from superparamagnetic materials, which exhibit magnetic moments in the presence of an external field. The most common magnetic NPs are made from iron oxides and have mean diameters around 5.0–30.0 nm (19,60). Despite the interesting properties of these inorganic NP-based contrast agents, neither quantum dots nor magnetic NPs can be used in X-ray imaging techniques. Given their specific characteristics, quantum dots are used in single- and multiphoton microscopy (i.e. non-X-ray dependent fluorescence imaging) (19,58,59,61,62), whereas magnetic NPs are used in MRI (19). For this reason, the majority of the attempts to develop novel inorganic NP-based X-ray contrast agents are focused on the utilization of elements with high atomic numbers.

Currently, there is an increasing trend towards replacing iodine with elements with higher X-ray absorption coefficients. Interest in iodine has declined not only because it has a moderate atomic number when it is compared with other elements, but also because it has a low K-shell binding energy of 33.18 keV (63,64). The K-edge is a sudden increase in the linear or mass X-ray absorption coefficient occurring at a characteristic energy just above the binding energy of the electrons in the K-shell of an atom (65). Therefore, iodine has suboptimal X-ray absorption coefficients at 100–130 kVp (19), which is the common X-ray tube potential range employed by many clinical imaging scanners. Despite the enormous variety of elements with higher atomic numbers than iodine, only a few of them have been extensively studied. As a matter of fact, most of the research has been focused on the use of gold (Au), a transition metal with excellent X-ray attenuation properties that can easily be used to prepare functionalized NPs (12,19,22). However, bismuth (Bi), lanthanides and tantalum (Ta) are becoming equally important because they are less expensive than gold. The K-edge and mass X-ray absorption coefficient at 100 keV of each of the aforementioned elements are summarized in Table 1. In an effort to create NP-based X-ray contrast agents with improved characteristics, many researchers are exploring the X-ray attenuation profiles and toxicity of the aforementioned elements. In the following sections, advancements and achievements in this field are discussed in detail.

Table 1. K-edge and mass X-ray absorption coefficient at 100 keV of elements utilized to produce nanoparticle-based X-ray contrast agents. The table summarizes the K-edge and mass X-ray absorption coefficient of iodine, barium, gadolinium, ytterbium, tantalum, gold and bismuth

Element	Chemical symbol	Atomic number	K-edge	Mass X-ray absorption coefficient at 100 keV
Iodine	I	53	33.17 keV	1.94 $cm^2\ g^{-1}$
Barium	Ba	56	37.44 keV	2.20 $cm^2\ g^{-1}$
Gadolinium	Gd	64	50.24 keV	3.11 $cm^2\ g^{-1}$
Ytterbium	Yb	70	61.33 keV	3.88 $cm^2\ g^{-1}$
Tantalum	Ta	73	67.42 keV	4.30 $cm^2\ g^{-1}$
Gold	Au	79	80.75 keV	5.16 $cm^2\ g^{-1}$
Bismuth	Bi	83	90.52 keV	5.74 $cm^2\ g^{-1}$

3.2.1. Gold nanoparticles

The reason why gold has garnered a lot of attention in the development of iodine-free NP-based X-ray contrast agents is because it possesses several properties that make it suitable for medical imaging applications. For example, it has a higher atomic number ($Z_{Au} = 79$) and a higher mass X-ray absorption coefficient (5.16 $cm^2\ g^{-1}$ at 100 keV) (22) than iodine. This means that gold provides about 2.7 times greater X-ray contrast per unit weight than iodine and, additionally, it has an optimal X-ray absorption coefficient at 80–100 keV, reducing interference from bone and soft tissue absorption (22). Another advantage of gold nanoparticles (AuNPs) is that they have been investigated for many years in other biological applications, where they exhibit good biotolerability and marginal levels of toxicity [LD_{50}, or median lethal dose, equal to 3.2 g of gold per kg (22)] (33,66). Additionally, owing to their small size, AuNPs readily travel through the microscopic capillaries of the circulatory system, facilitating intravenous use (33).

Given these unique properties, several gold nanostructures, including, but not limited to, nanorods, nanoclusters, nanoshells, nanocages, nanocubes and nanoprisms, have been prepared in addition to AuNPs (spherical shape) (53). The intrinsic properties of nanostructures made from metals are determined not only by their size, but also by their shape, composition, crystallinity and inner structure (solid or hollow) (67). The optical properties of gold nanostructures, for example, can be tuned by changing the shape (35), which is controlled mostly by the gold precursor concentration and the growth rate in a specific direction, influenced by the presence of ions in the reaction (68). A distinctive shape-dependent ultraviolet–visible, infrared and surface plasmon resonance spectroscopy behavior has been found before for gold nanostructures given that, depending on their shape, their maximum absorption peaks are shifted over hundreds of nanometers in wavelength (68,69). As a result, besides their applications in X-ray imaging, different gold nanostructures have been utilized for photothermal therapy, surface enhanced Raman scattering and photoacoustic tomography (35). To date, only spheres and rods have been evaluated as X-ray contrast agents. As long as the molar concentration of gold across the treatments is equal, no statistical significance difference is expected between the contrast enhancement of spheres and rods, which is in agreement with previous experimental findings (35,70). Thus, the differences between these two types of nanostructures may only rely on their biodistribution, which depends mainly on their size and size distribution, and their recognition by phagocytes. Basically, rods, and other elongated nanostructures, exhibit low uptake by MPS cells and, hence, prolonged circulation half-lives relative to spheres (71,72).

Given that AuNPs have been the object of intensive investigation for many years, their biodistribution, pharmacokinetics and pharmacodynamics are well understood. Recently, the contrast enhancement of a solution of AuNP with a mean diameter of 1.90 nm was compared with Ultravist® (iopromide, 300 mg of I per mL), a clinically approved iodinated contrast agent, at various X-ray tube potentials in an imaging phantom (33). In this experiment, 55 mg of lyophilized AuNP powder were suspended in 550 μL of deionized water and 1.08 mL of stock iopromide was diluted with 3.92 mL of deionized water. At an equal concentration of 0.51 M of the radiopaque element (i.e. either gold or iodine), an imaging study was performed at medium (40–80 kVp) and high (80–140 kVp) X-ray tube potentials using computed radiography (CR) and CT, respectively. It was observed that AuNP provided more contrast enhancement than the iodinated X-ray contrast agent (Fig. 6). However, the specific improvement reached by replacing iodine with gold as the radiopaque element was dependent on the X-ray tube potential utilized. For example, in the CR scans, the contrast enhancement was higher at low X-ray tube potentials (<50 kVp; Fig. 6A), whereas in the CT scans, it was higher at high X-ray tube potentials (>100 kVp; Fig. 6B) (33). This study showed that gold possesses high X-ray attenuation capabilities over a wide range of X-ray tube potentials, providing an imminent advantage over iodine.

Given the favorable X-ray attenuation results of gold, the toxicity of AuNPs has been evaluated in both *in vitro* and *in vivo* studies, showing that they can be used for medical applications. For instance, an MTT [3-(4,5-dimethylthiazol-2-yl)-2,5-diphenyltetrazolium bromide] assay was used to determine the cell viability of the K562 leukemia cell line after 3 days of continuous exposure to AuNPs of different sizes containing different surface modifiers (66). The AuNPs had mean diameters of 4 nm (capped with either cysteine residues or citrate), 12 nm (capped with glucose) and 18 nm (capped with citrate, biotin, or cetyltrimethylammonium bromide, CTAB). It was observed that all of the 4 and 12 nm AuNPs were not toxic at concentrations up to 25 μM, while the 18 nm AuNPs with citrate and biotin surface modifiers did not show cytotoxicity at concentrations up to 250 μM. Although the 18 nm CTAB-capped AuNPs exhibited significant toxicity at very low concentrations (<1.0 μM), the toxicity was associated with the presence of unbound CTAB. After removal of the unbound CTAB by centrifuging and washing the AuNPs with deionized water, a significant decrease in toxicity

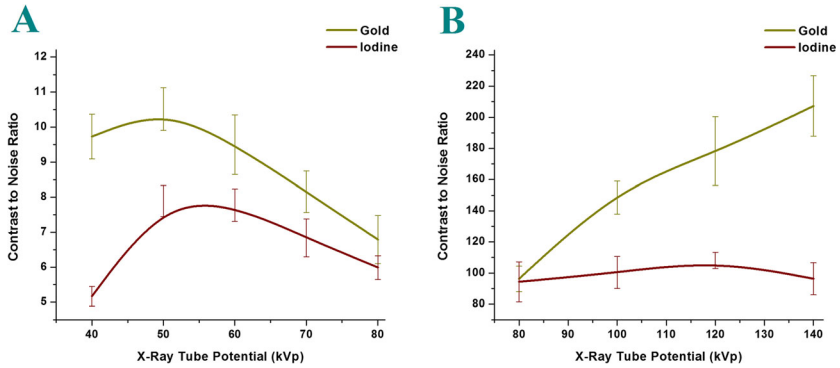

Figure 6. Comparison of the contrast-to-noise ratio of AuNPs and an iodine-based X-ray contrast agent at different X-ray tube potentials. The graphs show that the contrast-to-noise ratio of AuNPs and Ultravist® imaged by (A) CR and (B) CT is dependent on the X-ray tube potential applied. Adapted with permission from Jackson *et al*. (33).

was observed. Then, nuclear magnetic resonance (NMR) was used to corroborate that only unbound CTAB was removed from the AuNPs. For all the experiments, cell uptake was monitored by visible spectroscopy, revealing that the AuNPs are taken up by the cells without significant changes in size or morphology. These results proved that AuNPs are only toxic at very high concentrations, which are not employed in medical applications. Moreover, it was also demonstrated that the toxicity observed with the use of the CTAB-capped AuNPs was related to the precursor used, so that the NPs themselves are not necessarily detrimental to cellular function (66).

Most importantly, the toxicity of AuNPs with a mean diameter of 1.90 ± 0.10 nm was evaluated *in vivo* using 60 outbred CD1 mice (male and female). The mice were randomized into four groups. The first three groups received intravenous injections of the AuNP suspended in phosphate-buffered saline (PBS) at pH 7.4 at different concentrations (700, 70, and 7.0 mg of Au per kg), whereas the control group received an intravenous injection of just buffer. A histological examination of 24 vital organs and tissues from each mouse 30 days following injection showed no evidence of toxicity in any of the animals. Furthermore, the biodistribution and contrast enhancement were appraised by injecting buffered AuNPs at pH 4 into the tail vein of Balb/C mice bearing EMT-6 subcutaneous mammary tumors. The total volume injected was 0.01 mL per g of mouse weight at a concentration of 270 mg of Au per mL. For comparison purposes, the iodine-based X-ray contrast agent iohexol (Omnipaque^{TM}) was injected in another group of mice at the same concentration of the radiopaque element. After injection, the vascular system was imaged by planar projection using a clinical mammography unit. AuNPs allowed blood vessels with a mean diameter of 100 μm to be distinguished and imaging, detection and measurement of angiogenic and hypervascularized regions were also possible. Additionally, it was observed that the AuNPs cleared through the kidneys in less than 1 h and they did not accumulate in the liver and the spleen (Fig. 7) (22). The aforementioned results suggest that iodinated X-ray contrast agents and AuNPs differ in their pharmacokinetic properties.

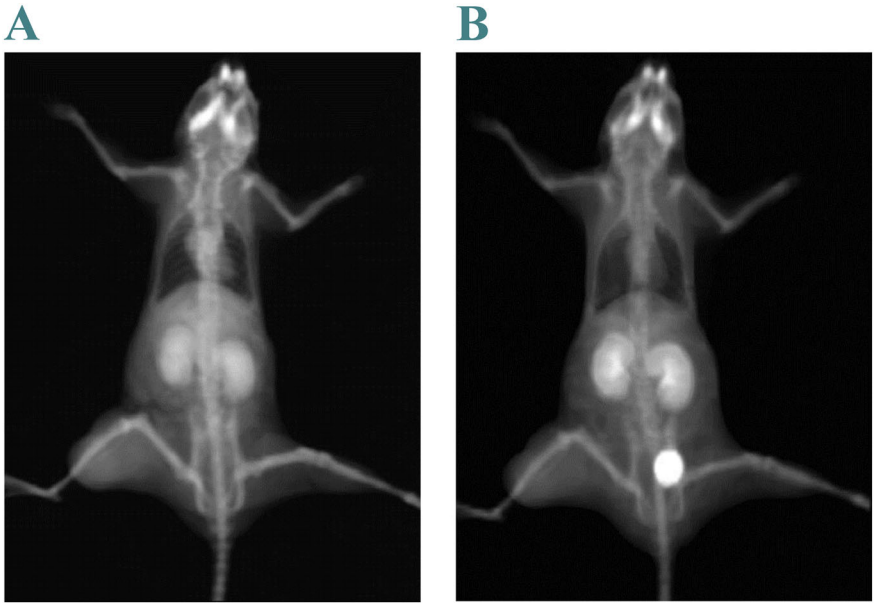

Figure 7. Biodistribution and contrast enhancement of AuNPs by planar imaging. Following administration into the tail vein of Balb/C mice bearing EMT-6 subcutaneous mammary tumors, 1.90 ± 0.10 nm AuNPs exhibited high contrast enhancement of angiogenic and hypervascularized regions for approximately 1 h and clearance through the kidneys and the bladder. The pictures depict the biodistribution of AuNPs (A) 2 and (B) 45 min after injection. Figure kindly provided by Dr. James F. Hainfeld.

The former are rapidly excreted through the kidneys, whereas the latter are extensively retained in tumors after blood clearance. For this reason, AuNPs may be useful for enhanced tumor detection and possibly for therapy if drugs are loaded into the NP core (19,22,48).

Even though AuNPs overcome some limitations of clinically used X-ray contrast agents, gold is more expensive than iodine, which can limit its utilization for large-scale applications. Consequently, other elements with high atomic numbers and biological tolerance have started to gain importance for the development of NP-based X-ray contrast agents.

3.2.2. *Bismuth nanoparticles*

Bismuth has become increasingly important during the last years not only because it has a high atomic number ($Z_{Bi} = 83$), but also because it decomposes to small and renally clearable Bi(III) species *in vivo* as a result of its tendency to oxidize and hydrolyze in water (52,73). Actually, it is well known that metallothionine, a cysteine-rich protein abundant in the kidneys, exhibits a preferential affinity for Bi(III) species and, therefore, enhances the clearance and urinary excretion of Bi(III) complexes (73). Nevertheless, the oxidative and hydrolytic instability of bismuth has extensively limited its use for diagnostic and molecular imaging applications in the form of NPs, as their production must be carried out in an anaerobic environment, using organic solvents (52,74).

Despite the aforementioned challenges, the production of stable bismuth glyconanoparticles (BiGNPs) was recently achieved using an aerobic method that requires the reduction of bismuth nitrate pentahydrate, which is a source of Bi(III) cations, by sodium borohydride ($NaBH_4$) in a pH-controlled aqueous solution (52). The synthesis of the NPs was performed with magnetic stirring at >800 rpm and 40 °C. Stabilization of the BiGNPs was possible after addition of dextran as a surface stabilizing ligand, as it imparts both oxidative and colloidal stability to the NPs when they are formed slowly (i.e. over a period of 1–10 min). As the solubility of bismuth nitrate pentahydrate is dependent on the pH of the reaction medium, particle aggregation was prevented by maintaining the pH between 8 and 10, a condition that maximizes the stability of the BiGNP. A pH <8 leads to the formation of large aggregates of BiGNP, whereas a pH >10 prevents the nucleation of the NPs since Bi(III) remains insoluble and, thus, is unavailable for reduction. The optimized BiGNPs had a mean diameter of 19.50 ± 3.70 nm (52). Although neither toxicity nor X-ray attenuation studies were performed, the BiGNPs produced by this method have size, solubility and stability characteristics that make them suitable for use as novel X-ray contrast agents. The simplicity of this method promises to open the way for the application of bismuth in diagnostic and molecular imaging applications, provided there is more evidence of the safety and efficacy of the bismuth-based NPs.

The synthesis of Bi_2S_3 NPs constitutes another important research area regarding the use of bismuth for diagnostic imaging applications, as Bi_2S_3 has been proven to exhibit low toxicity and rapid excretion *in vivo* (75). However, advances in this field are limited owing to the lack of methods to produce Bi_2S_3 NPs with a narrow size distribution. Although most research has been focused on the production of nanorods (76) and polydispersed nanocrystals (77) via a one-step hydrothermal method, a method to mass produce Bi_2S_3 NPs with a narrow size distribution has recently been reported (78). The method requires the injection of a solution of thioacetamide in oleyl amine into a solution of bismuth neodecanoate and oleic acid in octadecene at 105 °C. At this temperature, thioacetamide desulfurizes, which allows for the synthesis of Bi_2S_3. Bi_2S_3 NPs can then be recovered by a simple centrifugation step. Additionally, Bi_2S_3 NPs can be dispersed in a variety of organic solvents to modify their surface via a ligand exchange method. For example, in the same study, poly(vinylpyrrolidone) (PVP), a biocompatible polymer, was used to prepare 2–3 nm PVP-Bi_2S_3 NPs, suitable for the detection of liver metastases. These NPs showed high contrast enhancement and low toxicity *in vivo* (78).

3.2.3. *Lanthanide-doped nanoparticles*

The elements of the lanthanide series have been extensively used in MRI imaging. Gadolinium (Gd), for example, has been utilized over recent years owing to its chemical versatility to form complexes with different chelators (79–83). However, it has been reported that gadolinium enhances the development of CMN (84) and nephrogenic systemic fibrosis (32) at low concentrations and, therefore, much interest has recently focused on other lanthanides. Given the chemical and physical similarities between all the elements of the lanthanide series, the likelihood of praseodymium (Pr), europium (Eu) and holmium (Ho) to induce nephrogenic systemic fibrosis-like skin lesions in rats were recently evaluated. The study was carried out using lanthanide–diethylenetriamine pentaacetic–bismethylamide complexes. In all cases, the development of the disease was influenced by the concentration of the lanthanide detected in the skin (32).

Despite the toxicity associated with these rare-earth elements, lanthanides have a great deal of potential to be used in X-ray imaging techniques. All the elements of the lanthanide series have higher atomic numbers than iodine and, thus, are more effective in absorbing energetic photons of a polyenergetic spectrum (32). For example, gadolinium ($Z_{Gd} = 64$) has a mass X-ray absorption coefficient of 3.11 $cm^2\ g^{-1}$ at 100 keV (85), which is almost twice that of iodine. Therefore, in an attempt to exploit this characteristic, some of these elements have been encapsulated into NPs to develop a nontoxic lanthanide-based X-ray contrast agent. In previous studies, it has been observed that lanthanide-doped NPs are effectively taken up by cells. There is also evidence that human cells internalize these NPs by nonspecific endocytosis (86). Since the toxicity reported for lanthanides is caused by the release of lanthanide ions (32), the synthesis and encapsulation of more stable lanthanide complexes leads to an improved *in vivo* safety profile (32,87). Currently, an interesting area of research is the development of NPs with a core consisting of a mixture of lanthanides. Given the versatile properties of these rare-earth elements, these NPs can be used for multimodal imaging. Furthermore, the combination of a lanthanide with another radiopaque element in the same vehicle has recently given rise to the development of hybrid NP-based X-ray contrast agents. The promising applications of these two new-fashioned NPs are described below.

3.2.3.1. Multimodal and hybrid lanthanide-containing contrast agents. NPs comprising more than one lanthanide are valuable because of their multimodal properties. These NPs can be used not only in CT, but also in MRI and/or optical imaging, leading to additional information and synergistic advantages. For example, multimodal imaging facilitates the performance of pharmacokinetics studies, helps elucidating complex mechanisms of drug uptake and gives insight into processes that affect and influence tumor growth and behavior. Most of the research has been focused on

the utilization of erbium (Er; $Z_{Er} = 68$) (6,32), thulium (Tm; $Z_{Tm} = 69$) (32,85), ytterbium (Yb; $Z_{Yb} = 70$) (6,32,85) and even gadolinium (88). Given its excellent biocompatibility and high mass X-ray absorption coefficient (3.88 $cm^2\ g^{-1}$ at 100 keV), ytterbium is probably the most promising candidate for diagnostic and molecular imaging applications among all the elements of the lanthanide series (85).

For example, NPs with a solid Er^{3+}-doped Yb_2O_3 core and a pegylated shell (PEG-Yb_2O_3:Er^{3+} NPs) suitable for multimodal imaging have been recently designed and synthesized (6). The NPs were produced using a one-pot urea-based homogenous precipitation method. To functionalize the surface of the NPs with PEG chains, they were mixed and sonicated for 6 h with trialkoxysilylated *m*-PEG (silanated *m*-PEG) in deionized water. After this final step, the mean diameter of the PEG-Yb_2O_3:Er^{3+} NPs was 175 ± 32.60 nm. CT and upconversion fluorescence imaging studies performed in rats and mice, respectively, showed that a higher contrast enhancement is obtained with PEG-Yb_2O_3:Er^{3+} NPs than with iobitridol, a routinely used iodinated contrast agent. It was also found that the NPs mainly accumulated in the MPS, especially in the liver and the spleen, and were cleared in a stepwise manner, as suggested by the decrease in Yb^{3+} signal from the liver, spleen, kidneys, lungs and heart over a period of 30 days. Aside from the bright and well resolved images with long blood circulation time and effective enrichment in various organs, PEG-Yb_2O_3:Er^{3+} NPs demonstrated high biocompatibility in both *in vitro* and *in vivo* studies (6).

Owing to the inherent advantages of nanoparticles with bimodal imaging capabilities, another group recently prepared PEG-$NaYbF_4$:Tm^{3+} NPs using a simple stirring method (85). A solution of $RECl_3$ (where RE = 98% Yb^{3+} and 2% Tm^{3+}), water, oleic acid and 1-octadecane was mixed with a methanol solution of NH_4F and NaOH and stirred for 2 h. After methanol evaporation, the resulting solution was slowly heated to 280 °C and dispersed in cyclohexane to form NPs. Finally, the product was stirred with a PEG(5000)-SH aqueous solution over 24 h to render the otherwise hydrophobic surface of the nanoparticles hydrophilic. The PEG-$NaYbF_4$:Tm^{3+} NPs, with a mean diameter around 20 nm, exhibited both high *in vitro* and *in vivo* performance in CT and near-infrared fluorescence imaging compared with iobitridol. Furthermore, enhanced hepatic imaging was observed with the use of PEG-$NaYbF_4$:Tm^{3+} NPs owing to rapid uptake by phagocytic cells in the liver (Fig. 8). Hence, as a result of the passive targeting by the EPR effect in tumors, these NPs have interesting applications for imaging of hepatic tumors (85).

Related to multimodal contrast agents are hybrid NP-based X-ray contrast agents, which are synthesized by combining into a single carrier various elements with adequate X-ray attenuation capabilities but different K-edge values (55,89). As a result of the differential attenuation of X-ray photons, this strategy allows engineering X-ray contrast agents that provide optimal contrast enhancement at different X-ray tube potentials. This approach was recently followed to develop an NP-based X-ray contrast agent comprising both ytterbium and barium (Ba; $Z_{Ba} = 56$) (89), which is commonly used orally as barium sulfate ($BaSO_4$) for clinical gastrointestinal tract imaging (90–92). As depicted in Table 1, the K shell binding energies of ytterbium and barium are 61.33 and 37.44 keV, respectively. Hence, ytterbium provides a larger X-ray attenuation at higher X-ray tube potentials (>100 kVp), whereas barium provides larger X-ray attenuation at lower X-ray tube potentials (<100 kVp). First, a $BaYbF_5$ core was prepared by thermal decomposition of the corresponding trifluoroacetate precursors in oleic acid. Then, a pegylated silica shell was added to impart aqueous solubility to these inherently

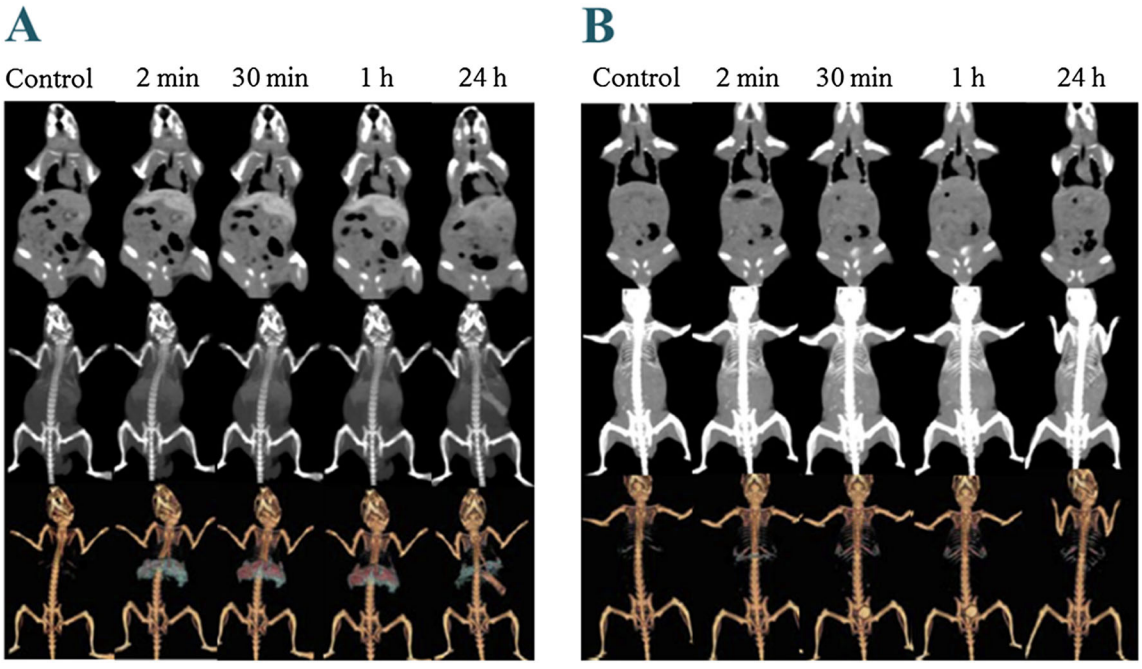

Figure 8. Comparison of the biodistribution and contrast enhancement of PEG-NaYbF4:Tm^{3+} NPs and an iodine-based X-ray contrast agent by CT imaging. The pictures show the biodistribution and contrast enhancement of (A) 20 nm PEG-NaYbF4:Tm^{3+} NPs and (B) iobitridol. The CT slices were acquired after an intravenous injection of 150 μL of either a physiological saline solution of PEG-NaYbF4:Tm^{3+} NPs (20 mg of Yb per mL) or iobitridol (25.6 mg of I per ml) into Kunming mice. The control refers to mice before injection. Top, serial CT coronal views; middle, maximum intensity projection; and bottom, 3D volume rendering CT images. Adapted with permission from Xing *et al.* (85).

hydrophobic structures, yielding hydrophilic PEG-SiO_3-$BaYbF_5$ NPs. As expected, this binary X-ray contrast agent maintained high X-ray attenuation properties from 80 to 140 kVp. Additionally, it exhibited an increased contrast enhancement relative to iobitridol and an NP-based X-ray contrast agent comprising a single radiopaque element previously synthesized and reported [PEG-$NaYbF_4$ NPs (93)]. Finally, this hybrid NP-based X-ray contrast agent showed high stability and biocompatibility both *in vivo* and *in vitro*. In summary, the utilization of this type of lanthanide-doped NPs has garnered much attention owing to their overall safety and potential used for diagnostic and molecular imaging applications. The aforementioned results give insight into the numerous advantages of using elements of the lanthanide series as X-ray contrast agents, particularly when they are combined with other radiopaque elements, which is currently an ongoing research. Lanthanide-doped NP-based X-ray contrast agents promise to become an alternative for patients that are contraindicated for iodinated X-ray contrast agents (19).

3.2.4. *Tantalum pentoxide nanoparticles*

Despite the success achieved with the production of NP-based X-ray contrast agents using gold, bismuth or lanthanides, other elements with high atomic numbers have also been studied in an attempt to find a more suitable contrast agent for diagnostic and molecular imaging scans in terms of safety and efficacy. Tantalum ($Z_{Ta} = 73$), a transition metal, is of particular interest when it reacts with oxygen to form tantalum pentoxide (Ta_2O_5) (19,94). The reasons why Ta_2O_5 has become the focus of attention are related to its high solubility in water, chemical stability and biocompatibility (94). Owing to its excellent X-ray attenuation properties, Ta_2O_5 has been used before as an X-ray contrast agent for tracheobronchial imaging (19,95), in which it has usually been delivered as a powder aerosol via the trachea (95). In order to develop a formulation suitable for an intravenous administration, Ta_2O_5 NPs were recently designed and analyzed (94).

Basically, the NPs comprised a Ta_2O_5 core coated with (2-diethylphosphato-ethyl)triethoxysilane (94). The mean diameter was around 6 nm and they remained stable over a period of 6 months in an aqueous solution. Following the injection of the NPs in rats, it was evident that they possessed better X-ray attenuation properties than iopromide at an equivalent concentration. Ta_2O_5 NPs exhibited a prolonged blood pool residence time and were eventually taken up by MPS cells in both the liver and the spleen. Moreover, an *in vitro* toxicity study performed in RAW264.7 cells demonstrated that none of the rats showed toxic effects over a period of 2 weeks post-injection (94). Together, these results indicate that water-soluble Ta_2O_5 NPs could be used for diagnostic and molecular imaging applications. However, it is important to perform more imaging and safety studies to corroborate the applicability of these NPs as novel X-ray contrast agents. Further research in this field might lead to the design and preparation of optimized, targeted Ta_2O_5 NPs.

4. CONCLUSION AND OUTLOOK

The design, production and evaluation of NP-based X-ray contrast agents comprising mainly elements with high atomic numbers is a straightforward strategy to improve clinically used iodinated X-ray contrast agents. Several studies have demonstrated that these nanoparticulate systems exhibit longer blood circulation times, lower toxicity and, most importantly, enhanced X-ray attenuation capabilities. Furthermore, the characteristic high surface area-to-volume ratio of the NPs is advantageous to add a high number of ligands to their surface, increasing the specificity and overall efficiency of diagnostic and molecular imaging procedures. Thus, NP-based X-ray contrast agents usually have tunable biodistribution profiles that are controlled not only by the size and size distribution of the NPs, but also by the targeting moieties attached to their surface.

Given the copious advantages of designing X-ray contrast agent carriers at the nanoscale and the simplicity of the most common methods to produce NPs (i.e. emulsion polymerization and nanoprecipitation), one of the first attempts to reduce the adverse effects associated with the administration of small iodinated molecules during X-ray scans was the production of iodine-loaded NPs. Despite the successful preparation of these nanoparticulate systems and the low toxicity observed after their utilization, the recent trend is to replace iodine with high atomic number elements, which are known to exhibit excellent X-ray attenuation capabilities. Gold became one of the first prospects to prepare iodine-free NP-based X-ray contrast agents because it possesses a high biotolerability and a low cytotoxicity, characteristics that make it suitable for use for biological applications (22,33,66). Moreover, bismuth, erbium, thulium, ytterbium and tantalum have recently become the focus of attention for the production of NPs not only because they all exhibit good X-ray attenuation properties, but also because they are inexpensive in comparison with gold (19).

Although significant progress has been made in preparing stable NP-based X-ray contrast agents from elements with better X-ray attenuation properties than iodine, it is still necessary to conduct more research regarding the effect of the size and size distribution of the NPs on their X-ray absorption capabilities. It is well known that particle size is very important in drug delivery applications mainly for two reasons. First, it determines the final site of particle accumulation within the body. Second, it influences the release profile of the cargo. The size distribution, on the other hand, determines the extent of trapping (96,97). Even though there is not a clear-cut relationship between these two properties and the contrast enhancement in X-ray imaging, it is reasonable to expect a differential X-ray absorption owing to differences in the release profile of the contrast generating material from NPs of different sizes. Recently, the contrast enhancement of <5 and >30 nm AuNPs was appraised at X-ray tube potentials ranging from 40 to 100 kVp. Although no statistical significance difference was found between the contrast-to-noise ratio values of these samples of NPs, and even between samples with different shapes (spheres and rods), it was found that the concentration of the radiopaque element plays a pivotal role in the X-ray absorption process (70). As the concentration decreases as the radiopaque element is released from the NP, it is now important to assess the biodegradation rate of NPs of different sizes made from a variety of polymers. However, this type of study has not been conducted yet.

The potential of the functionalization of the NP surface with targeting moieties is another research field that has not been appropriately exploited. Despite the fact that the attachment of biological ligands to NP-based X-ray contrast agents promises to increase the specificity of medical and molecular imaging procedures, only a few research groups have reported the successful incorporation of targeting moieties to this novel type of X-ray contrast agents. For example, AuNPs conjugated with a monoclonal antibody that selectively targets the CD4 receptor, which is highly expressed on the surface of T cells and macrophages, have been recently synthesized and imaged effectively in mice (98). Given

the potential of this targeted NP-based X-ray contrast agents to diagnose, treat and monitor diseases, more research in this field is expected to be conducted in the future.

The NP-based X-ray contrast agents presented throughout this review summarize the advances made to develop contrast agents with enhanced X-ray attenuation properties and reduced toxicity. However, as nanomedicine is a field that is developing at a highly accelerated rate, we should definitely expect more improvements over the following years. Fortunately, our understanding of the relationship between the structure, physicochemical properties, efficiency and toxicity of X-ray contrast agents is improving. This information can be used to develop 'smart' NP-based contrast agents that will provide higher resolutions at lower concentrations, reducing the adverse effects and costs associated with imaging procedures and enhancing, at the same time, patient welfare during diagnoses.

Acknowledgment

The authors would like to thank Dr. Kevin Letchford of the Faculty of Pharmaceutical Sciences at UBC in Vancouver, Canada for scientific discussion throughout the preparation of this work. We gratefully acknowledge Dr. James F. Hainfeld for kindly providing the figure depicting the biodistribution of AuNPs in mice (i.e. Fig. 7). José Carlos De La Vega would also like to thank the National Council of Science and Technology (CONACyT) of Mexico for funding and support.

REFERENCES

1. Skotland T, Iversen T-G, Sandvig K. New metal-based nanoparticles for intravenous use: Requirements for clinical success with focus on medical imaging. Nanomed Nanotechnol 2010; 6(6): 730–737.
2. Massoud TF, Gambhir SS. Molecular imaging in living subjects: Seeing fundamental biological processes in a new light. Genes Dev 2003; 17(5): 545–580.
3. Khan FM. The physics of radiation therapy. Lippincott Williams & Wilkins: Philadelphia, PA, 1994.
4. Gundogdu O, Nirgianaki E, Che Ismail E, Jenneson PM, Bradley DA. Benchtop phase-contrast X-ray imaging. Appl Radiat Isot 2007; 65 (12): 1337–1344.
5. Loudos G, Kagadis GC, Psimadas D. Current status and future perspectives of *in vivo* small animal imaging using radiolabeled nanoparticles. Eur J Radiol 2011; 78(2): 287–295.
6. Liu Z, Li Z, Liu J, Gu S, Yuan Q, Ren J, Qu X. Long-circulating Er^{3+}-doped Yb_2O_3 up-conversion nanoparticle as an *in vivo* X-ray CT imaging contrast agent. Biomaterials 2012; 33(28): 6748–6757.
7. Hallouard F, Anton N, Choquet P, Constantinesco A, Vandamme T. Iodinated blood pool contrast media for preclinical X-ray imaging applications – A review. Biomaterials 2010; 31(24): 6249–6268.
8. Ritman EL. Current status of developments and applications of micro-CT. Annu Rev Biomed Eng 2011; 13(1): 531–552.
9. Kallai I, Mizrahi O, Tawackoli W, Gazit Z, Pelled G, Gazit D. Microcomputed tomography-based structural analysis of various bone tissue regeneration models. Nat Protoc 2011; 6(1): 105–110.
10. Ritman EL. Micro-computed tomography – Current status and developments. Annu Rev Biomed Eng 2004; 6(1): 185–208.
11. Cormode DP, Skajaa T, Fayad ZA, Mulder WJM. Nanotechnology in medical imaging: Probe design and applications. Arterioscler Thromb Vasc Biol 2009; 29(7): 992–1000.
12. Chien C-C, Chen H-H, Lai S-F, Wu K-C, Cai X, Hwu Y, Petibois C, Chu Y, Margaritondo G. Gold nanoparticles as high-resolution X-ray imaging contrast agents for the analysis of tumor-related micro-vasculature. J Nanobiotechnol 2012; 10(1): 1–12.
13. Misri R, Saatchi K, Häfeli UO. Nanoprobes for hybrid SPECT/MR molecular imaging. Nanomedicine 2012; 7(5): 719–733.
14. Saatchi K, Soema P, Gelder N, Misri R, McPhee K, Baker JHE, Reinsberg SA, Brooks DE, Häfeli UO. Hyperbranched polyglycerols as trimodal imaging agents: Design, biocompatibility, and tumor uptake. Bioconjug Chem 2012; 23(3): 372–381.
15. Ganguly A, Wen Z, Daniel BL, Butts K, Kee ST, Rieke V, Do HM, Pelc NJ, Fahrig R. Truly hybrid X-ray/MR imaging: Toward a streamlined clinical system. Acad Radiol 2005; 12(9): 1167–1177.
16. Fukushima K, Bravo PE, Higuchi T, Schuleri KH, Lin X, Abraham MR, Xia J, Mathews WB, Dannals RF, Lardo AC, Szabo Z, Bengel FM. Molecular hybrid positron emission tomography/computed tomography imaging of cardiac angiotensin II type 1 receptors. J Am Coll Cardiol 2012; 60(24): 2527–2534.
17. Hussain T, Nguyen QT. Molecular imaging for cancer diagnosis and surgery. Adv Drug Deliv Rev 2014; 66(0): 90–100.
18. Krause W, Schneider P. Chemistry of X-ray contrast agents. Springer: Berlin, 2002.
19. Lusic H, Grinstaff MW. X-ray computed tomography contrast agents. Chem Rev 2013; 113(3): 1641–1666.
20. Zhou S-A, Brahme A. Development of phase-contrast X-ray imaging techniques and potential medical applications. Phys Med 2008; 24(3): 129–148.
21. Williams IM, Siu KKW, Runxuan G, He X, Hart SA, Styles CB, Lewis RA. Towards the clinical application of X-ray phase contrast imaging. Eur J Radiol 2008; 68(3, suppl): 73–77.
22. Hainfeld JF, Slatkin DN, Focella TM, Smilowitz HM. Gold nanoparticles: A new X-ray contrast agent. Br J Radiol 2006; 79(939): 248–253.
23. Wynn DG, Humphries G, Morisson-Iveson V, Nairne J, Newington IM, Passmore J, Wistrand L-G. The synthesis and evaluation of unsymmetrical dimeric X-ray contrast agents. Tetrahedron Lett 2011; 52(24): 3068–3071.
24. Newington IM, Humphries G, Lasbistes N, Morisson-Iveson V, Nairne J, Passmore J, Thanning M, Wistrand L-G, Wynn D. The synthesis and evaluation of trimeric X-ray contrast agents. Tetrahedron Lett 2011; 52(24): 3065–3067.
25. Jost G, Lenhard DC, Sieber MA, Lengsfeld P, Huetter J, Pietsch H. Changes of renal water diffusion coefficient after application of iodinated contrast agents: Effect of viscosity. Invest Radiol 2011; 46(12): 796–800.
26. Pasternak JJ, Williamson EE. Clinical pharmacology, uses, and adverse reactions of iodinated contrast agents: A primer for the non-radiologist. Mayo Clin Proc 2012; 87(4): 390–402.
27. Todd B. Iodine-based contrast agents. Geriatr Nurs 1987; 8(6): 341–348.
28. Speck U. Contrast agents: X-ray contrast agents and molecular imaging – A contradiction? Springer: Berlin, 2008.
29. Bohren CF, Huffman DR. Absorption and scattering of light by small particles. John Wiley & Sons: Weinheim, 1983.
30. Mullan BF, Madsen MT, Messerle L, Kolesnichenko V, Kruger J. X-ray attenuation coefficients of high-atomic-number, hexanuclear transition metal cluster compounds: A new paradigm for radiographic contrast agents. Acad Radiol 2000; 7(4): 254–259.
31. Ahn S, Jung SY, Lee JP, Lee SJ. Properties of iopamidol-incorporated poly(vinyl alcohol) microparticle as an X-ray imaging flow tracer. J Phys Chem B 2011; 115(5): 889–901.
32. Pietsch H, Jost G, Frenzel T, Raschke M, Walter J, Schirmer H, Hütter J, Sieber MA. Efficacy and safety of lanthanoids as X-ray contrast agents. Eur J Radiol 2011; 80(2): 349–356.
33. Jackson PA, Rahman WNWA, Wong CJ, Ackerly T, Geso M. Potential dependent superiority of gold nanoparticles in comparison to iodinated contrast agents. Eur J Radiol 2010; 75(1): 104–109.
34. Wharton T, Wilson LJ. Toward fullerene-based X-ray contrast agents: Design and synthesis of non-ionic, highly-iodinated derivatives of C_{60}. Tetrahedron Lett 2002; 43(4): 561–564.
35. Lee N, Choi SH, Hyeon T. Nano-sized CT contrast agents. Adv Mater 2013; 25(19): 2641–2660.
36. Torchilin VP. PEG-based micelles as carriers of contrast agents for different imaging modalities. Adv Drug Deliv Rev 2002; 54(2): 235–252.
37. Letchford K, Burt H. A review of the formation and classification of amphiphilic block copolymer nanoparticulate structures: Micelles, nanospheres, nanocapsules and polymersomes. Eur J Pharm Biopharm 2007; 65(3): 259–269.
38. Allen C, Maysinger D, Eisenberg A. Nano-engineering block copolymer aggregates for drug delivery. Colloids Surf B 1999; 16(1–4): 3–27.
39. Havron A, Seltzer SE, Davis MA, Shulkin P. Radiopaque liposomes: A promising new contrast material for computed tomography of the spleen. Radiology 1981; 140(2): 507–511.
40. Desser TS, Rubin DL, Muller H, McIntire GL, Bacon ER, Toner JL. Blood pool and liver enhancement in CT with liposomal Iodixanol: Comparison with iohexol. Acad Radiol 1999; 6(3): 176–183.
41. Mukundan S, Ghaghada KB, Badea CT, Kao C-Y, Hedlund LW, Provenzale JM, Johnson GA, Chen E, Bellamkonda RV, Annapragada A.

A liposomal nanoscale contrast agent for preclinical CT in mice. AJR 2006; 186(2): 300–307.
42. Badea CT, Samei E, Ghaghada K, Saunders R, Yuan H, Qi Y, Hedlund LW, Mukundan S. Utility of a prototype liposomal contrast agent for X-ray imaging of breast cancer: A proof of concept using micro-CT in small animals. In Proceedings of SPIE. Medical Imaging 2008. Physics of Medical Imaging: San Diego, CA, 2008; 6913: 691303–691309.
43. Trubetskoy VS, Gazelle GS, Wolf GL, Torchilin VP. Block-copolymer of polyethylene glycol and polylysine as a carrier of organic iodine: Design of long-circulating particulate contrast medium for X-ray computed tomography. J Drug Targeting 1997; 4(6): 381–388.
44. Torchilin VP, Frank-Kamenetsky MD, Wolf GL. CT visualization of blood pool in rats by using long-circulating, iodine-containing micelles. Acad Radiol 1999; 6(1): 61–65.
45. Fu Y, Nitecki DE, Maltby D, Simon GH, Berejnoi K, Raatschen H-J, Yeh BM, Shames DM, Brasch RC. Dendritic iodinated contrast agents with PEG-cores for CT imaging: Synthesis and preliminary characterization. Bioconjug Chem 2006; 17(4): 1043–1056.
46. Cormode DP, Naha PC, Fayad ZA. Nanoparticle contrast agents for computed tomography: A focus on micelles. Contrast Media Mol Imag 2014; 9(1): 37–52.
47. Tran V-T, Benoît J-P, Venier-Julienne M-C. Why and how to prepare biodegradable, monodispersed, polymeric microparticles in the field of pharmacy? Int J Pharm 2011; 407(1–2): 1–11.
48. Cho EC, Glaus C, Chen J, Welch MJ, Xia Y. Inorganic nanoparticle-based contrast agents for molecular imaging. Trends Mol Med 2010; 16(12): 561–573.
49. Mulder WJM, Griffioen AW, Strijkers GJ, Cormode DP, Nicolay K, Fayad ZA. Magnetic and fluorescent nanoparticles for multimodality imaging. Nanomedicine 2007; 2(3): 307–324.
50. Peng C, Zheng L, Chen Q, Shen M, Guo R, Wang H, Cao X, Zhang G, Shi X. PEGylated dendrimer-entrapped gold nanoparticles for *in vivo* blood pool and tumor imaging by computed tomography. Biomaterials 2012; 33(4): 1107–1119.
51. Ahmed N, Fessi H, Elaissari A. Theranostic applications of nanoparticles in cancer. Drug Discov Today 2012; 17(17–18): 928–934.
52. Brown AL, Goforth AM. pH-dependent synthesis and stability of aqueous, elemental bismuth glyconanoparticle colloids: Potentially biocompatible X-ray contrast agents. Chem Mater 2012; 24(9): 1599–1605.
53. Dreaden EC, Alkilany AM, Huang X, Murphy CJ, El-Sayed MA. The golden age: Gold nanoparticles for biomedicine. Chem Soc Rev 2012; 41(7): 2740–2779.
54. Debbage P, Jaschke W. Molecular imaging with nanoparticles: Giant roles for dwarf actors. Histochem Cell Biol 2008; 130(5): 845–875.
55. Liu Y, Ai K, Lu L. Nanoparticulate X-ray computed tomography contrast agents: From design validation to *in vivo* applications. Acc Chem Res 2012; 45(10): 1817–1827.
56. Aviv H, Bartling S, Kiesslling F, Margel S. Radiopaque iodinated copolymeric nanoparticles for X-ray imaging applications. Biomaterials 2009; 30(29): 5610–5616.
57. Mawad D, Mouaziz H, Penciu A, Méhier H, Fenet B, Fessi H, Chevalier Y. Elaboration of radiopaque iodinated nanoparticles for *in situ* control of local drug delivery. Biomaterials 2009; 30(29): 5667–5674.
58. Gao X, Yang L, Petros JA, Marshall FF, Simons JW, Nie S. *In vivo* molecular and cellular imaging with quantum dots. Curr Opin Biotechnol 2005; 16(1): 63–72.
59. Gao X, Cui Y, Levenson RM, Chung LWK, Nie S. *In vivo* cancer targeting and imaging with semiconductor quantum dots. Nat Biotech 2004; 22(8): 969–976.
60. Andrä W, Häfeli U, Hergt R, Misri R. Application of magnetic particles in medicine and biology. In Handbook of Magnetism and Advanced Magnetic Materials, Kronmüller H, Parkin SP (eds.). John Wiley & Sons: Chichester, 2007; 2536–2568.
61. Gao J, Chen K, Xie R, Xie J, Lee S, Cheng Z, Peng X, Chen X. Ultrasmall near-infrared non-cadmium quantum dots for *in vivo* tumor imaging. Small 2010; 6(2): 256–261.
62. Chan WCW, Maxwell DJ, Gao X, Bailey RE, Han M, Nie S. Luminescent quantum dots for multiplexed biological detection and imaging. Curr Opin Biotechnol 2002; 13(1): 40–46.
63. Hoheisel M. Review of medical imaging with emphasis on X-ray detectors. Nucl Instrum Methods Phys 2006; 563(1): 215–224.
64. NIST Physical Measurement Laboratory. X-ray transition energy: K-edge table, 1996.
65. Gillam JE, Kitcher D, Beveridge TE, Midgley S, Hall C, Lewis RA. K-edge subtraction using an energy-resolving position-sensitive detector. Nucl Instrum Methods Phys 2009; 604(1–2): 97–100.
66. Connor EE, Mwamuka J, Gole A, Murphy CJ, Wyatt MD. Gold nanoparticles are taken up by human cells but do not cause acute cytotoxicity. Small 2005; 1(3): 325–327.
67. Sun Y, Xia Y. Shape-controlled synthesis of gold and silver nanoparticles. Science 2002; 298(5601): 2176–2179.
68. Kim F, Connor S, Song H, Kuykendall T, Yang P. Platonic gold nanocrystals. Angew Chem Int Ed 2004; 116(28): 3759–3763.
69. Oldenburg SJ, Averitt RD, Westcott SL, Halas NJ. Nanoengineering of optical resonances. Chem Phys Lett 1998; 288(2–4): 243–247.
70. Jackson P, Periasamy S, Bansal V, Geso M. Evaluation of the effects of gold nanoparticle shape and size on contrast enhancement in radiological imaging. Australas Phys Eng Sci Med 2011; 34(2): 243–249.
71. Park J-H, von Maltzahn G, Zhang L, Schwartz MP, Ruoslahti E, Bhatia SN, Sailor MJ. Magnetic iron oxide nanoworms for tumor targeting and imaging. Adv Mater 2008; 20(9): 1630–1635.
72. Champion JA, Mitragotri S. Role of target geometry in phagocytosis. Proc Natl Acad Sci USA 2006; 103(13): 4930–4934.
73. Sun H, Li H, Harvey H, Sadler PJ. Interactions of bismuth complexes with metallothionein(II). J Biol Chem 1999; 274(41): 29094–29101.
74. Wang F, Tang R, Yu H, Gibbons PC, Buhro WE. Size- and shape-controlled synthesis of bismuth nanoparticles. Chem Mater 2008; 20(11): 3656–3662.
75. Rabin O, Manuel Perez J, Grimm J, Wojtkiewicz G, Weissleder R. An X-ray computed tomography imaging agent based on long-circulating bismuth sulphide nanoparticles. Nat Mater 2006; 5(2): 118–122.
76. Liu Z, Fang J, Xu W, Xu X, Wu S, Zhu X. Low temperature hydrothermal synthesis of Bi_2S_3 nanorods using BiOI nanosheets as self-sacrificing templates. Mater Lett 2012; 88: 82–85.
77. Li Y, Wei F, Ma Y, Zhang H, Gao Z, Dai L, Qin G. Selected-control hydrothermal synthesis and photoresponse properties of Bi_2S_3 micro/nanocrystals. Cryst Eng Commun 2013; 15(33): 6611–6616.
78. Ai K, Liu Y, Liu J, Yuan Q, He Y, Lu L. Large-scale synthesis of Bi_2S_3 nanodots as a contrast agent for *in vivo* X-ray computed tomography imaging. Adv Mater 2011; 23(42): 4886–4891.
79. Choppin GR, Schaab KM. Lanthanide(III) complexation with ligands as possible contrast enhancing agents for MRI. Inorg Chim Acta 1996; 252(1–2): 299–310.
80. Comblin V, Gilsoul D, Hermann M, Humblet V, Jacques V, Mesbahi M, Sauvage C, Desreux JF. Designing new MRI contrast agents: A coordination chemistry challenge. Coord Chem Rev 1999; 185–186(0): 451–470.
81. Bonnet CS, Tóth É. Towards highly efficient, intelligent and bimodal imaging probes: Novel approaches provided by lanthanide coordination chemistry. C R Chim 2010; 13(6–7): 700–714.
82. Yan G-P, Zheng C-Y, Cao W, Li W, Li L-Y, Liu M-L, Zhang Y-X, Zhuo R-X. Synthesis and preliminary evaluation of gadolinium complexes containing sulfonamide groups as potential MRI contrast agents. Radiography 2003; 9(1): 35–41.
83. Zhou X, Yang L, Yan G, Xu W, Zhou C, Zhang Q, Li L, Liu F, Guo J, Zhao Q. Dopamine-containing gadolinium complex as magnetic resonance imaging contrast agent. J Rare Earths 2012; 30(9): 884–889.
84. Elmståhl B, Nyman U, Leander P, Chai C-M, Frennby B, Almén T. Gadolinium contrast media are more nephrotoxic than a low osmolar iodine medium employing doses with equal X-ray attenuation in renal arteriography: An experimental study in pigs. Acad Radiol 2004; 11(11): 1219–1228.
85. Xing H, Bu W, Ren Q, Zheng X, Li M, Zhang S, Qu H, Wang Z, Hua Y, Zhao K, Zhou L, Peng W, Shi J. A $NaYbF_4$: Tm^{3+} nanoprobe for CT and NIR-to-NIR fluorescent bimodal imaging. Biomaterials 2012; 33(21): 5384–5393.
86. Vancaeyzeele C, Ornatsky O, Baranov V, Shen L, Abdelrahman A, Winnik MA. Lanthanide-containing polymer nanoparticles for biological tagging applications: Nonspecific endocytosis and cell adhesion. J Am Chem Soc 2007; 129(44): 13653–13660.
87. Stouwdam JW, Hebbink GA, Huskens J, van Veggel FCJM. Lanthanide-doped nanoparticles with excellent luminescent properties in organic media. Chem Mater 2003; 15(24): 4604–4616.
88. Liu Y, Chen Z, Liu C, Yu D, Lu Z, Zhang N. Gadolinium-loaded polymeric nanoparticles modified with anti-VEGF as multifunctional MRI contrast agents for the diagnosis of liver cancer. Biomaterials 2011; 32(22): 5167–5176.

89. Liu Y, Ai K, Liu J, Yuan Q, He Y, Lu L. Hybrid $BaYbF_5$ nanoparticles: Novel binary contrast agent for high-resolution *in vivo* X-ray computed tomography angiography. Adv Healthcare Mater 2012; 1(4): 461–466.
90. Summers DS, Roger MD, Allan PL, Murchison JT. Accelerating the transit time of barium sulphate suspensions in small bowel examinations. Eur J Radiol 2007; 62(1): 122–125.
91. Périard MA. Adverse effects and complications related to the use of barium sulphate contrast media for radiological examinations of the gastrointestinal tract: A literature review. Canadian Journal of Medical Radiation Technology 2003; 34(3): 3–9.
92. O'Connor SD, Summers RM. Revisiting oral barium sulfate contrast agents. Acad Radiol 2007; 14(1): 72–80.
93. Liu Y, Ai K, Liu J, Yuan Q, He Y, Lu L. A high-performance ytterbium-based nanoparticulate contrast agent for *in vivo* X-ray computed tomography imaging. Angew Chem Int Ed 2012; 51(6): 1437–1442.
94. Bonitatibus JPJ, Torres AS, Goddard GD, FitzGerald PF, Kulkarni AM. Synthesis, characterization, and computed tomography imaging of a tantalum oxide nanoparticle imaging agent. Chem Commun 2010; 46(47): 8956–8958.
95. Nadel JA, Wolfe WG, Graf PD. Powdered tantalum as a medium for bronchography in canine and human lungs. Invest Radiol 1968; 3(4): 229–238.
96. De La Vega JC, Elischer P, Schneider T, Häfeli UO. Uniform polymer microspheres: Monodispersity criteria, methods of formation and applications. Nanomedicine 2013; 8(2): 265–285.
97. Häfeli UO, Saatchi K, Elischer P, Misri R, Bokharaei M, Labiris NRe, Stoeber B. Lung perfusion imaging with monosized biodegradable microspheres. Biomacromolecules 2010; 11(3): 561–567.
98. Eck W, Nicholson AI, Zentgraf H, Semmler W, Bartling SN. Anti-CD4-targeted gold nanoparticles induce specific contrast enhancement of peripheral lymph nodes in X-ray computed tomography of live mice. Nano Lett 2010; 10(7): 2318–2322.

